# Use of Remote Sensing Observations to Study the Urban Climate on Tropical Coastal Cities

**Ana J. Picón-Feliciano and Ramón Vásquez,**
Department of Electrical and Computer Engineering, University of Puerto Rico, Mayagüez, Mayagüez, Puerto Rico
ana.picon@ece.uprm.edu

**Jorge González,**
Department of Mechanical Engineering, Santa Clara University
Santa Clara, USA

**Jeff Luvall & Douglas Rickman,**
NASA Global Hydrology and Climate Center, Huntsville
Alabama, USA

### Abstract

Local climate change effects due to urban growth have been characterized by great continental cities. This research is focused in the study of similar local climate effects due to urbanization in tropical coastal cities. With the use of remote sensing technology, climate changes due to urban growth can be detected. Airborne sensors can provide high resolution images that can be analyzed to identify the different components of the surface energy budget. The clearest local indicator of climate changes due to urban growth is an urban/rural convective circulation known as Urban Heat Islands (UHI). The main scientific objective of this research is to investigate the impact of the fast urbanization in the local climate of tropical coastal cities that is related to UHI. A field campaign was designed and executed in February 2004 to validate this phenomenon. The field campaign included measurements with on-board high resolution infrared (IR) sensors, ground weather stations, and upper air radiosonde balloons. The experimental campaign was denominated San Juan ATLAS Mission. The Airborne Thermal and Land Applications Sensor (ATLAS) from NASA/Stennis that operates in the visual and IR bands was used as the main sensor for this field campaign with the objective of investigating the Urban Heat Island (UHI) in San Juan, Puerto Rico. Temperatures as high as 60 °C over the developed areas differ from temperatures over vegetated areas of more than 30 °C during daytime. Results from this research have shown outstanding evidence of elevated surface temperatures over the urban landscape and clearly validate the development of UHI in San Juan, Puerto Rico.

*Keywords*: urban heat island, surface temperature, albedo, energy budget, ATLAS.

## Resumen

Los efectos de cambios climáticos locales por causa del crecimiento urbano han sido caracterizados en las grandes ciudades continentales. Esta investigación está enfocada en estudiar los diferentes efectos climáticos locales causados por la urbanización en ciudades tropicales-costeras. Con el uso de tecnología de percepción remota se pueden detectar los cambios climáticos causados por la urbanización en ciudades tropicales-costeras. Censores en el aire pueden proveer imágenes de alta-resolución que pueden ser analizadas para identificar los componentes diferentes de la energía en la superficie. Los indicadores locales más claros en cambios de clima por causa del crecimiento urbano son la circulación de tipo de convección de ciudad conocido como “Urban Hear Islands” (UHI). El objetivo científico principal de este estudio es investigar el impacto de la urbanización rápida en el clima local de ciudades tropicales-costeras que esté relacionado con el “UHI”. Una campaña fue diseñada y ejecutada en febrero de 2004 para validar este fenómeno. Esta campaña incluyó medidas en censores de alta-resolución Infra-rojos (IR), estaciones de clima, y globos de radio-sonda. La campaña experimental fue denominada Misión ATLAS de San Juan. El “Airborne Thermal and Land Applications Sensor” (ATLAS) de la NASA/Stennis que opera en las bandas visuales y de IR fue usado como sensor principal en este estudio de campo con el objetivo de investigar el “UHI” en San Juan, Puerto Rico. Temperaturas tan altas como 60 ºC o más en las áreas desarrolladas difieren de la temperatura en áreas con más vegetación, las cuales tenían más de 30 ºC durante el día. Los resultados de esta investigación han probado las evidencias de la temperatura de la superficie sobre el paisaje urbano y evidentemente validan el desarrollo de UHI en San Juan, Puerto Rico.

*Palabras Clave:* Isla urbana de calor, temperatura de la superficie, albedo, presupuesto de energía, ATLAS.

## Introduction

It is difficult to imagine that cities in small tropical islands show local climate change effects similar to those in great continental cities. It was recently discovered by González, J. E., Luvall, J. C., Rickman, D., Comarazamy, D. E. & Picón, A. J. (2006) that this might be the case for the city of San Juan, Puerto Rico, a relatively affluent coastal tropical city of nearly 2 million inhabitants. The main scientific objective of this research is to investigate the relationship between urban growth, land cover change, and the development of the urban heat island phenomenon over a tropical coastal city; San Juan, Puerto Rico. Also, study the overall effects of urban development on surface energy budget characteristics across the urban landscape through time at nested spatial scales from local to regional. A field campaign was designed and executed in February 2004 to validate this phenomenon. The field campaign included measurements with on-board high resolution infrared (IR) sensors, ground weather stations, and upper air radiosonde balloons. The Airborne Thermal and Land Applications Sensor (ATLAS) from NASA/Stennis that operates in the visual and IR bands was used as the main sensor for this field campaign with the objective of investigating the Urban Heat Island (UHI) in San Juan, Puerto Rico. Infrared sensor measurements can provide land surface parameters such as temperature and albedo. These two parameters are the key elements in the study of urban heat island. A brief review of relevant works is provided in this section. Landsat 7 has been used in urban heat island studies in the city of Atlanta (Poreh, M., 1996). This sensor has a spatial resolution of 60 m in the spectral range of 10.40 to 12.5 µm. One constraint of the instrument is the temporal variation due to overpasses through Puerto Rico which is every 16 days. To retrieve surface temperature, band 6 is adjusted with an atmospheric model or profile.

Fukui, Y., Hirose, Y. & Mushiake, N. (2002) presented a study based on the surface temperature distribution and the urban structure in Tokyo using the Advanced Spaceborne Thermal Emission and Reflection Radiometer (ASTER) and LIDAR data. ASTER has a spatial resolution of 90 m in the spectral range of 8.125 to 8.825µm, 8.925 to 9.275µm and 10.25 to 11.65µm. In this study, two different scenes from ASTER were used to calculate the surface temperature via the temperature/emissivity separation (TES) algorithm. The correlation of the surface temperature and the urban structure shows the impact of green areas on the urban heat environment and the falling of surface temperature in tall buildings during daytime and increasing of surface temperature during nighttime.

Furthermore, NOAA's Advanced Very High Resolution Radiometer (AVHRR) thermal IR images have been studied to understand the urban microclimates of cities such as Paris and Los Angeles (Dousset, B. & Gourmelon, F., 2001). This radiometer has a spatial resolution of 1 km and two thermal bands in the spectral range of 10.3 to 11.3µm and 11.5 to 12.5µm. To retrieve surface temperature, it uses a split window equation. NASA's Moderate Resolution Imaging Spectroradiometer (MODIS) has the same resolution as AVHRR but has the capability of acquiring data over 36 spectral bands. McCabe, M.F., Prata, A.J. & Kalma, J. D. (2001) compared MODIS and AVHRR land surface temperatures with ground based infrared thermometry measurements made in Tomago, Sandbeds, north of Newcastle, Australia. Comparisons show good agreement between MODIS, AVHRR and the infrared thermometer. Quattrochi, D. & Luvall, J. C. (2004) explain in detail the surface temperature retrieval from these instruments. No major research has been reported where remote sensing images are used to investigate the urban climate in tropical and subtropical regions.

The remaining parts of the paper are organized as follow: Section II presents the theoretical aspects and the post-processing of the ATLAS data, Section III presents results obtained from the San Juan area, Section IV includes the conclusions and the future work, and finally, Section V includes the references.

## Energy Surface Budget Definitions and ATLAS Data Post-Processing

The Airborne Thermal and Land Applications Sensor (ATLAS) of NASA/Stennis operates in the visual and infrared bands. The ATLAS can detect 15 multispectral channels of the radiation through the visible, near infrared, and thermal spectrums (see Figure 1). The sensor also incorporates the active sources of calibration needed for all bands. The data is corrected for the atmospheric radiation, and georectified before the analysis of the data is performed. The ATLAS sensor has been used in other field campaigns to investigate the UHI in Atlanta, Salt Lake City, Baton Rouge, and Sacramento, all in the continental mass of the United States of North America (Luvall, J.C., Rickman, D., Quattrochi, D. & Estes, M., 2005).

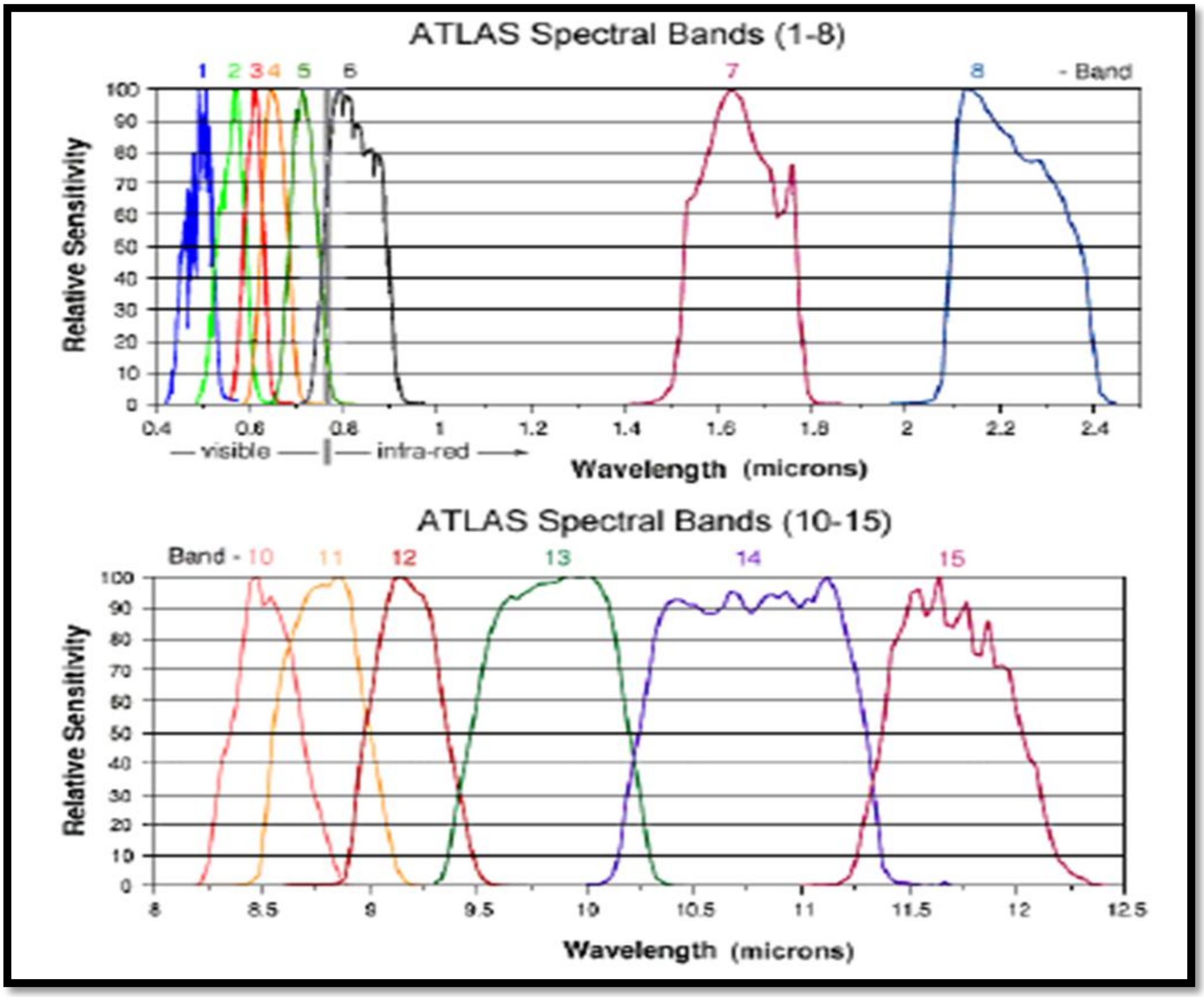

Figure 1. Spectral resolution of the airborne thermal and land applications sensor(ATLAS) from NASA/Stennis.

The ATLAS Mission of San Juan, Puerto Rico was conducted during February of 2004 to investigate the impact of the urban growth and landscape in the climate of this tropical city. The flight plan of the mission covered the metropolitan area within San Juan, the national forest of “El Yunque” to the east of San Juan, the city of Mayagüez in the west coast of Puerto Rico, and the Arecibo Radio Observatory located in the north central coast, for a total of 25 flight lines. The downtown area of San Juan, Hato Rey, was covered in a horizontal resolution of 5 meters in flights during the day and during the night. The remaining areas of the city were covered in a horizontal resolution of 10 meters. The flights were executed between the 11th and the 16th of February of 2004. In order to analyze the existence of an urban heat island in San Juan, and to support the data of the ATLAS sensor, several experimental campaigns for data collection were designed and conducted by different teams, in addition diverse numerical experiments were performed that helped to understand the phenomenon and its characteristics. The atmospheric corrections needed to produce calibrated data sets from ATLAS involve a complex procedure. They require direct measurements of the atmosphere extinction coefficients by wavelength and profiles of atmospheric temperatures and water vapor. ATLAS instrument characteristics and calibration are also required.

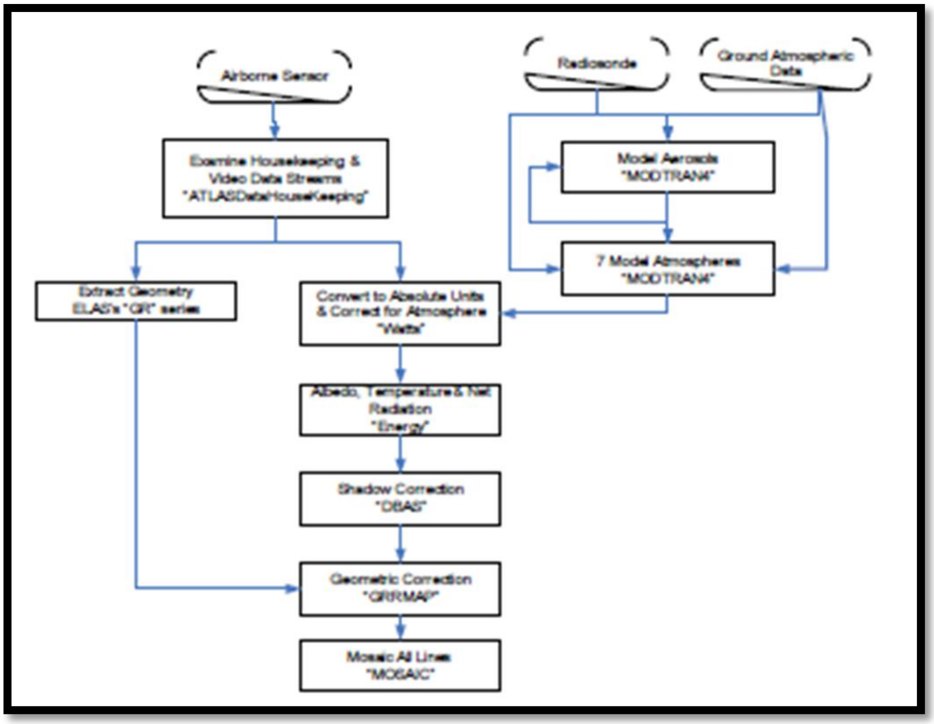

Figure 2. ATLAS overall data-processing flow.

Figure 2 details the process flow followed for this project including the images that resulted from every relevant routine. A combination of software was used for the processing, including the public domain image processing/remote sensing package ELAS (Beverley, A.M. & Penton, P.G., 1989) and a series of custom programs, Watts and Energy from ELASII (Rickman, D.L., Luvall, J. C. & Schiller, S., 2000).

MODTRAN4 (Berk, A., Anderson, G. P., Acharya, P. K., Chetwynd, J., Bernstein, L. S., Shettle, E. P., Matthew, M. W. & Adler-Golden, S. M., 1999) was used to model the atmospheric radiance and transmittance using input from radiosonde data and shadow band radiometers. Rickman, D.L., Luvall, J. C. & Schiller, S. (2000) details the procedure for calibrating the ATLAS sensor to produce the system transfer function to convert digital values (DV) into radiance measurements. These procedures produce ATLAS data files that are in physical units of energy. These files are used for the generation of files which derive albedo and surface temperature.

Surface temperature is a major component of the surface energy budget. Oke, T.R. (1987) presents the use of energy terms in modeling surface energy budgets allows the direct comparison of various land surfaces encountered in a landscape, from vegetated (forest and herbaceous) to non-vegetated (bare soil, roads, and buildings). The partitioning of energy budget terms depends on the surface type. In natural landscapes, the partitioning is dependent on canopy biomass, leaf area index, aerodynamic roughness, and moisture status, all of which are influenced by the development stage of the ecosystem. In urban landscapes, coverage by man-made materials substantially alters the surface energy budget. Figure 3 details the equations used to determine the net all-wave radiation balance (W/m$^2$) of landscape canopies (Oke, T.R., 1987).

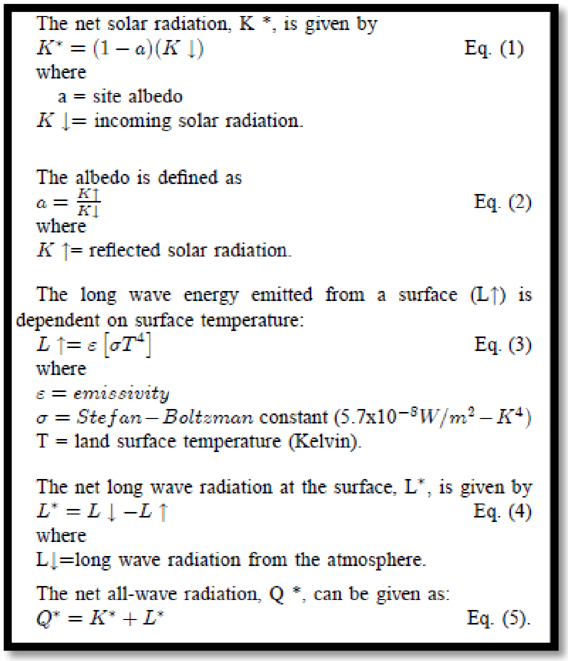

The net solar radiation, K *, is given by

$K^* = (1 - a)(K\downarrow)$ Eq. (1)

where

a = site albedo

$K\downarrow$= incoming solar radiation.

The albedo is defined as

$a = \frac{K\uparrow}{K\downarrow}$ Eq. (2)

where

$K\uparrow$= reflected solar radiation.

The long wave energy emitted from a surface (L↑) is dependent on surface temperature:

$L\uparrow = \varepsilon\left[\sigma T^4\right]$ Eq. (3)

where

$\varepsilon = emissivity$

$\sigma = Stefan - Boltzman$ constant ($5.7\text{x}10^{-8} W/m^2 - K^4$)

T = land surface temperature (Kelvin).

The net long wave radiation at the surface, L$^*$, is given by

$L^* = L\downarrow - L\uparrow$ Eq. (4)

where

L↓=long wave radiation from the atmosphere.

The net all-wave radiation, Q *, can be given as:

$Q^* = K^* + L^*$ Eq. (5).

Figure 3. Equations needed to determine the net all-wave radiation balance (W/m$^2$) of landscape canopies.

Net radiation (Q*), under most conditions, represents the total amount of energy available to the land surface for partitioning into non-radiative processes (mass heating, biological synthesis, etc.) at the surface. It is the amount of energy the system holds on to and degrades. In vegetated areas the amount of net radiation is dependent upon vegetation type and varies with canopy leaf area and structure. Figure 4 details the equation used to express the net radiation (Q*) as the sum of several non-radiative fluxes, such as: sensible heat flux (H), latent heat of vaporization of water (λ), transpiration flux (E) and energy flux into or out of storage (G).

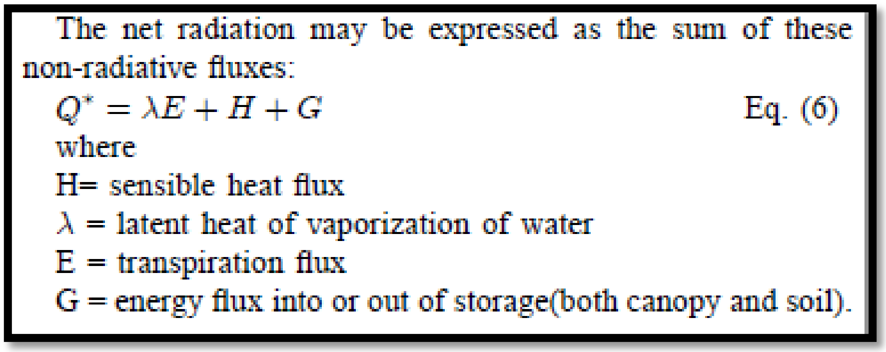

The net radiation may be expressed as the sum of these non-radiative fluxes:

$$Q^* = \lambda E + H + G \qquad \text{Eq. (6)}$$

where

H= sensible heat flux

$\lambda$ = latent heat of vaporization of water

E = transpiration flux

G = energy flux into or out of storage(both canopy and soil).

Figure 4. Equation used to express the net radiation as the sum of several non-radiative fluxes.

The partitioning of the net radiation between these non-radiative fluxes (λE, H and G) are also dependent on the makeup of the surface. Both the physiological control of moisture loss (stomatal resistance) and leaf/canopy morphology for vegetation determines how Q* is partitioned among λE, H, and G. For urban surfaces the coverage of both man-made materials and vegetation results in a heterogeneous mixture of surfaces which determine the partitioning of energy. The ATLAS sensors data allows the measurement of important terms in the radiative surface energy budget: reflected solar radiation (K↑) and the long wave energy emitted from a surface (L↑) on an urban landscape scale. When combined with output from MODTRAN4 atmospheric radiance models the remaining terms and Q* can be determined.

## Results Obtained from San Juan, Puerto Rico, including the Downtown Area of Hato Rey

During Flight 1 and Flight 5 of the mission, Hato Rey and the whole San Juan surface temperatures were obtained from the ATLAS sensors. With the use of ENVI$^{TM}$ and Matlab$^{TM}$ software, energy files from Hato Rey were manipulated to visualize and to determine the frequency distributions from the observed surface data. Flight lines 23 and 24 covered the area of Hato Rey at a resolution of 5 meters during the daytime. By looking at the surface temperatures from the mosaic of flight line 23 and flight line 24 (see Figure 5), urbanized areas can easily be identified. Lakes and vegetated areas are the coldest compared to the warmest roof tops and paved areas. It can be notice the large temperature differences between Northeast Hato Rey and Northwest Hato Rey. Northeast Hato Rey shows the coldest temperatures over the entire Hato Rey area. A significant urbanized area around Northwest Hato Rey can be seen in the thermal mosaic with warmer temperatures.

Figure 5. Mosaic of retrieved surface temperatures for “Hato Rey” Flight 1, lines 23 and 24. Surface temperatures are measured in degrees Celsius.

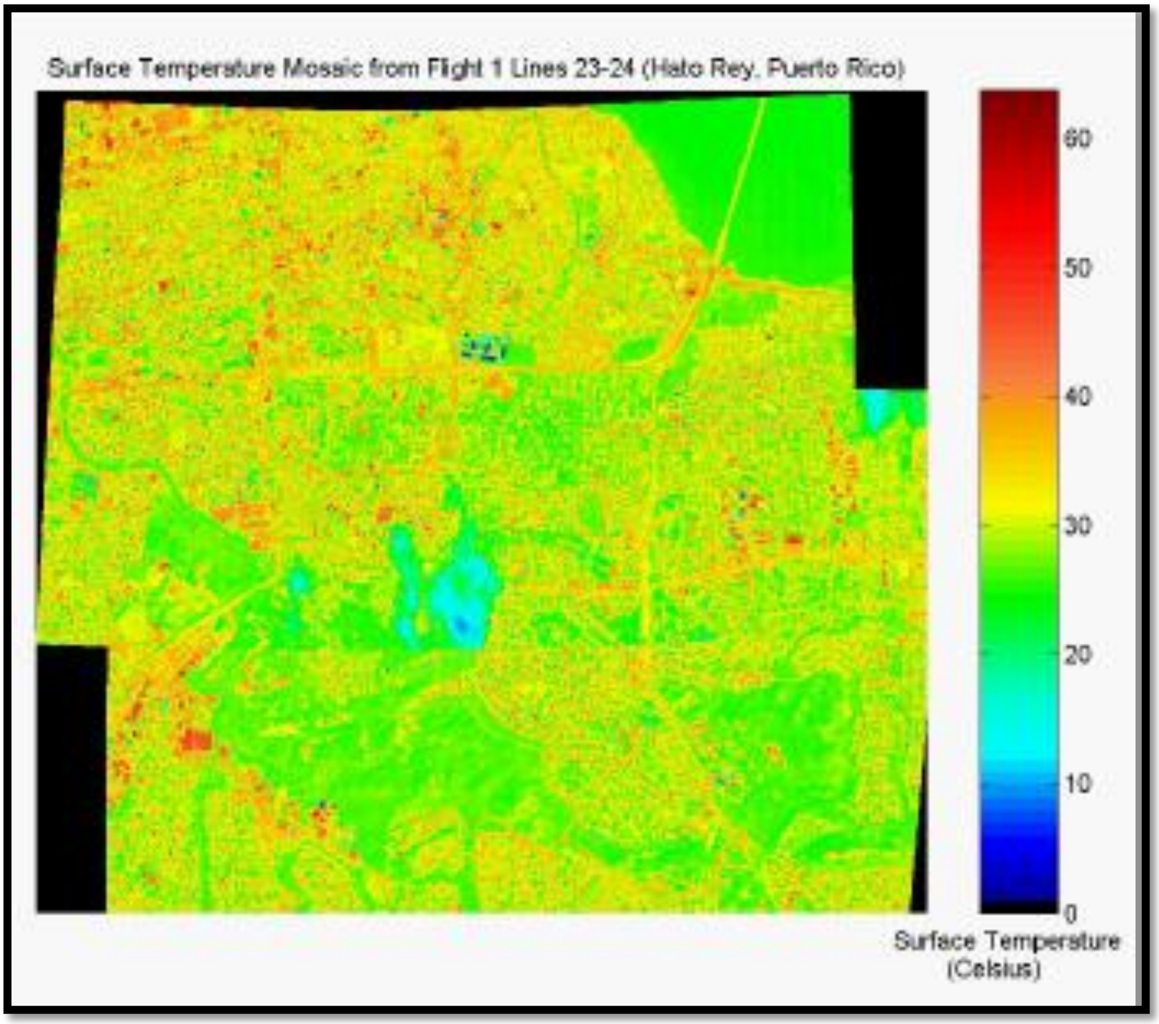

The temperature frequency distribution for flight line 24 (Figure 6) identifies important land surface features that make up the thermal fabric of the city. First, the San José Lagoon is identifiable by its peak as the coldest surface of 24.7 °C. The next coldest peak identifies the vegetated component near the Río Piedras Experimental Station around 27.2 °C. The hottest surface is associated to roofs and asphalt pavements and is represented by the "tail" of the distribution between 49.9 °C and 63.7 °C.

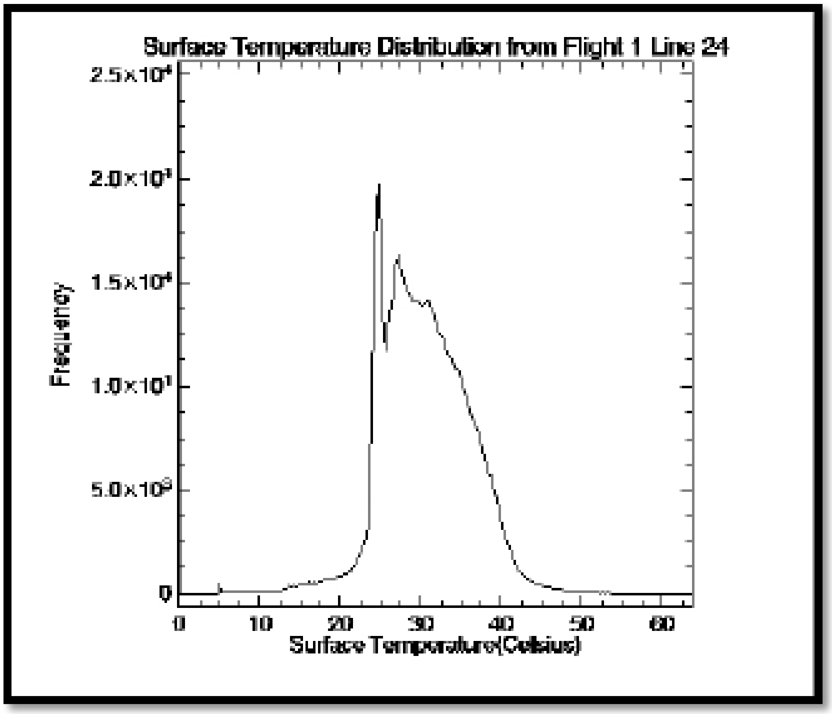

Figure 6. Frequency distribution of surface temperature for Hato Rey for Flight 1, line 24.

Albedo (K↑/K↓), the ratio of reflected (K↑) to incoming (K↓) solar radiation, does not truly reflect how the lands' surface partitions energy. A good example is the comparison between vegetated and asphalt surfaces. Both surfaces have a low albedo, but the asphalt surface temperature can be over 34 °C greater than the vegetated surface. If the surface temperature is included the needed additional information to assess the "urban fabric" of the city is provided. The surface temperature and albedo classifications represent a functional classification of that surface, that can readily be incorporated into the surface parameterization of meteorological and air quality models. Within each city, each land use has a unique "energy print" that is directly physically related to how that surface is processing energy. These "energy prints" of the land use are unique for each city.

In Figure 7, it is shown a scatter plot of surface temperature versus albedo for flight line 24. As it can be seen, the relation between surface temperature and albedo indicates the energy print of that portion of Hato Rey. Red pixels show the highest frequency of occurrences for a given pixel value of temperature and albedo, whereas the blue pixels show the lowest frequency. The lower left corner in the scatter plot identifies the dark and cool water bodies in the flight line 24. The upper side of the scatter plot identifies the light and hot buildings and paved areas. Because these.”energy prints” of the land use are unique for each city, a scatter from one city will differ significantly from the scatter plot of another city. Results from the scatter plot empathize that classifications based on cover type/land use cannot be applied across a variety of cities, since they cannot represent the true energy partitioning of that surface.

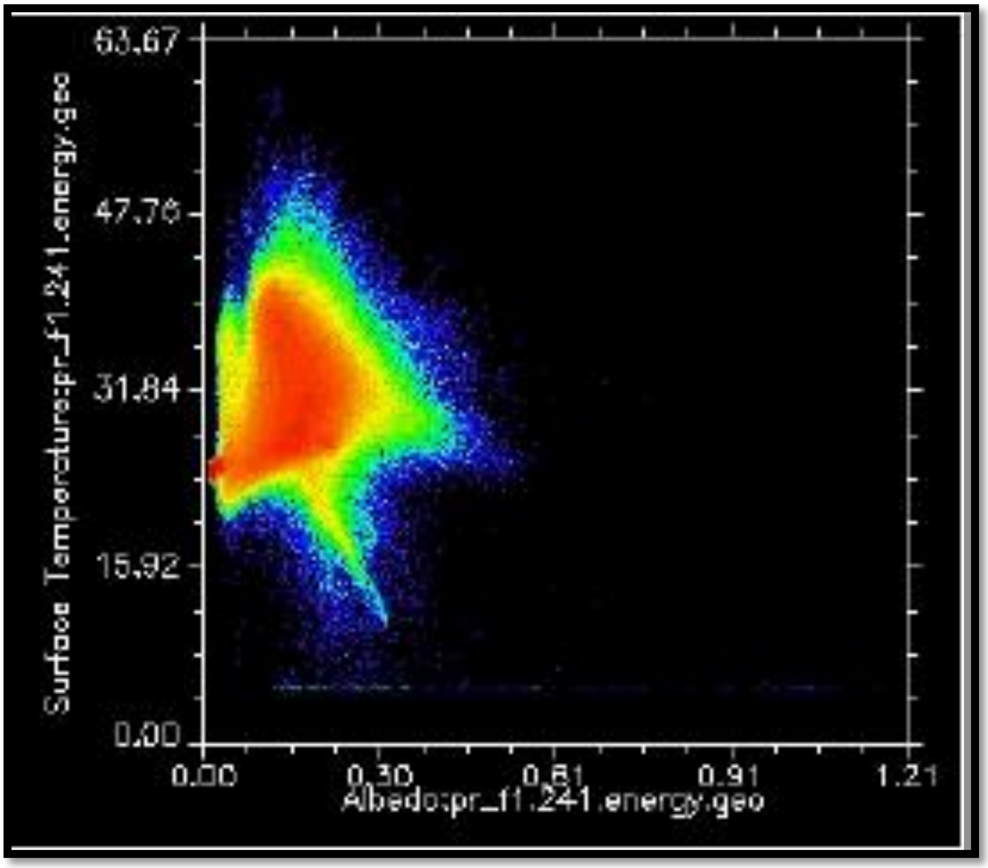

Figure 7. Scatter plot of surface temperature versus albedo for Hato Rey for Flight 1, line 24.

The San Juan Metropolitan zone includes vegetated areas such as the Río Piedras Experimental Station, lagoon, airport, coastal industrial areas such as Cataño and central building areas. The following figures correspond to the integration of San Juan flight lines. Figures 8, 9 and 10 show the composite mosaic of San Juan, the retrieved surface temperatures and the retrieved albedo, respectively. Differences in temperatures indicate a heat pattern dominating urban and coastal areas. Vegetated areas reflect albedo values around 0.07 and 0.15. Water bodies reflect albedo values around 0.06 and 0.3. Albedo values higher than 0.78 correspond to cloud bodies.

Figure 8. Composite mosaic of visible images for San Juan covering ten flight lines at a resolution of 10 meters.

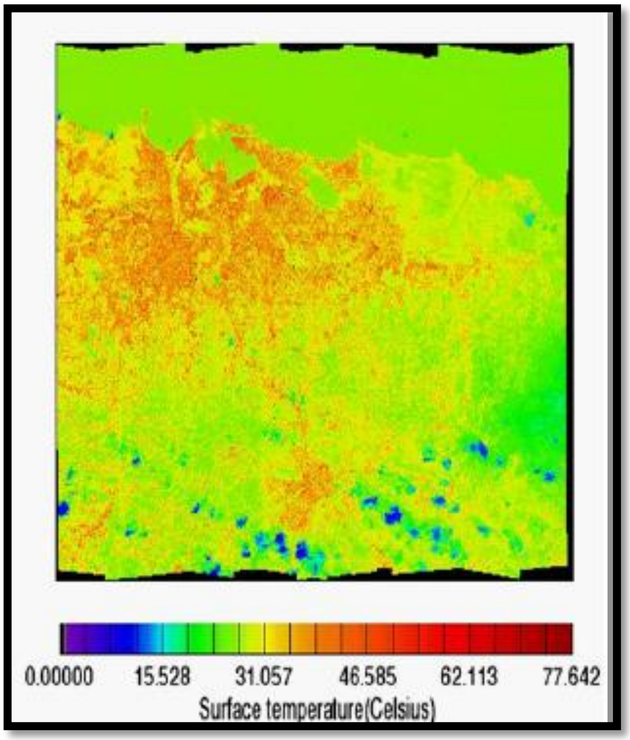

Figure 9. Mosaic of retrieved surface temperatures for San Juan Flight 5, lines 8 through 17. Surface temperatures are measured in degrees Celsius.

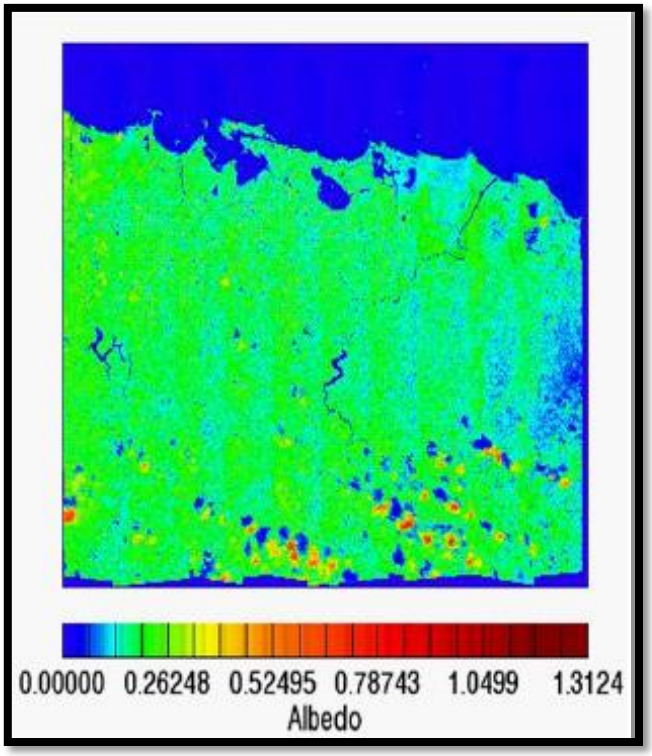

Figure 10. Mosaic of retrieved albedo for San Juan Flight 5, lines 8 through 17.

Since the San Juan Metropolitan zone includes vegetation, water bodies, residential, industrial and central building components, the surface energy budget can be evaluated by observing the energy contribution of each component to the whole UHI energy print. The way each surface partitions energy is unique depending on material type, vegetated or non-vegetated, water status, atmospheric vapor deficits, and the relative mixtures and arrangements of the various components of that surface. Figure 11 shows an image of San Juan with its relative surface energy components. Individual vegetated components such as the Río Piedras Experimental Station Area which is one of the most vegetated areas in the city shows a very low contribution of surface temperature versus albedo. Generally the industrial areas had the highest albedo and the hottest temperatures in contrast with the park areas that had lower albedo (not always the lowest) and lowest temperatures. Residential areas reflect low albedos in a range from low to high surface temperatures. The airport area is mostly an asphalt surface that can be very hot in terms of temperature. The hottest surfaces correlate with roofs and asphalt pavements.

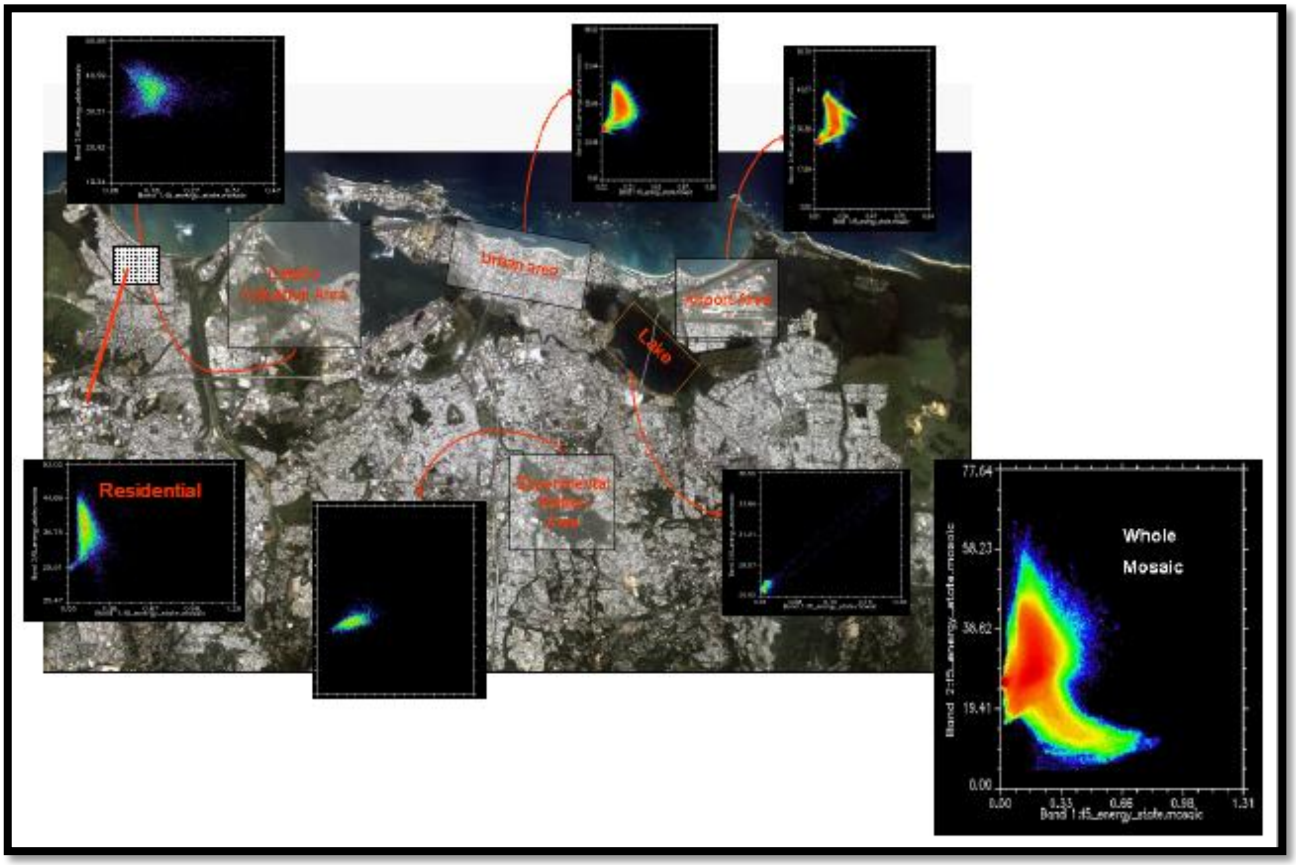

Figure 11. San Juan scatter plots that identifies the energy portions from urbanized and vegetated areas at different spots.

## Conclusions and Future Work

The work presented is part of a comprehensive investigation of the impact of land use for urbanization on the environment of a city located on a small tropical island, in this case, San Juan, Puerto Rico. The ATLAS field campaign conducted in February 2004 validates the development of UHI showing temperatures as high as 60 °C with temperature differences between the developed and vegetated areas of more than 30 °C during daytime. The thermal energy print of a large urban development is clearly observed from the high-resolution remote sensing images. Also, ATLAS has superior spectral resolution within the thermal IR channels. These offer the potential to make accurate measurements of thermal responses for different landscape characteristics and their corresponding land-atmosphere interactions over small wavelength regions. Energy prints from the different components in a urban city represent the surface energy portion that contributes to the total surface energy budget. Future work will include more comparisons in terms of surface energy budget that will be made by looking at other UHI cities, being either continental or mid-latitude locations.

## References

Berk, A., Anderson, G. P., Acharya, P. K., Chetwynd, J. Bernstein, L. S., Shettle, E. P., Matthew, M. W. & Adler-Golden, S. M. (1999) MODTRAN4 Users Manual. Air Force Research Laboratory, Space Vehicles Directorate, Air Force Material

Beverley, A.M. & Penton, P.G. (1989) ELAS, Earth Resources Laboratory Applications Software Vol II, User Reference; Earth Resources Lab. Report No. 183; NSTL, Mississippi, USA.

Dousset, B. & Gourmelon, F. (2001) Remote sensing applications to the analysis of urban microclimates. IEEE/ISPRS Joint Worshop Remote Sensing and Data Fusion over Urban Areas, 168-172.

Fukui, Y., Hirose, Y. & Mushiake, N. (2002) A study on the surface temperature distribution and the urban structure in Tokyo with ASTER and LIDAR data. Proceedings of Geoscience and Remote Sensing Symposium (IGARSS ’02), 4, 24-28.

González, J. E., Luvall, J. C., Rickman, D., Comarazamy, D. E. & Picón, A. J. (2006) Urban heat Island an a Coastal Tropical City: Case Study In The Metropolitan Area Of San Juan, Puerto Rico, Book chapter in Urban Remote Sensing, CRC Press, and D. Quattrochi Q. Weng and D. Quattrochi, Editors.

Luvall, J. C., Rickman, D., Quattrochi, D. & Estes, M. (2005) Aircraft Based Remotely Sensed Albedo and Surface Temperatures for Three US Cities; Color Roofing: Cutting through the Glare, Roof Consultants Institute Foundation, May 12-13, 2005, Atlanta, GA.; 8 pp.

McCabe, M.F., Prata, A.J. & Kalma, J. D. (2001) The Effects of Scale on Predictions of Land Surface Temperature from a variety of Remote Sensing Platforms. Proceedings of Geoscience and Remote Sensing Symposium (IGARSS '01), 3, 9-13.

Oke, T.R. (1987) Boundary Layer Climates. Cambridge University Press. 450 pp.

Poreh, M. (1996) Investigation of heat islands using small scale models, Atmospheric Environment, 30, 467-474.

Quattrochi, D. & Luvall, J. C. (2004) *Thermal Remote Sensing in Land Surface Processes*, CRC Press, ISBN 0415302242.

Rickman, D.L., Luvall, J. C. & Schiller, S. (2000) An algorithm to atmospherically correct visible and thermal airborne imagery. Workshop on Multi/Hyperspectral Technology and Applications, Redstone Arsenal, Alabama. Command, Anscom AFB, MA 01731-3010.

**Citación de este artículo:**

Picón-Feliciano, A. J., Vásquez, R., González, J., Luvall, J. & Rickman, D. (2009). Use of Remote Sensing Observations to Study the Urban Climate on Tropical Coastal Cities. *Revista Umbral*, 1, 218-232. Disponible en http://ojs.uprrp.edu/index.php/umbral/article/download/31/19

**Producción y Recursos en Internet:**

Producción de Umbral, Facultad de Estudios Generales, Universidad de Puerto Rico, Río Piedras. Disponible en http://umbral.uprrp.edu/revista